

STABILITY OF CURVED INTERFACES IN THE PERTURBED TWO-DIMENSIONAL ALLEN-CAHN SYSTEM

DAVID IRON*, THEODORE KOLOKOLONIKOV*, JOHN RUMSEY*, AND JUNCHENG
WEI†

Abstract. We consider the singular limit of a perturbed Allen-Cahn model on a bounded two dimensional domain:

$$\begin{cases} u_t = \varepsilon^2 \Delta u - 2(u - \varepsilon a)(u^2 - 1), & x \in \Omega \subset \mathbb{R}^2 \\ \partial_n u = 0, & x \in \partial\Omega \end{cases}$$

where ε is a small parameter and a is an $O(1)$ quantity. We study equilibrium solutions that have the form of a curved interface. Using singular perturbation techniques, we fully characterize the stability of such an equilibrium in terms of a certain geometric eigenvalue problem, and give a simple geometric interpretation of our stability results. Full numerical computations of the time-dependent PDE as well as of the associated two-dimensional eigenvalue problem are shown to be in excellent agreement with the analytical predictions.

Key words. Allen-Cahn equation, interface motion, spectral analysis, matched asymptotic expansions

1. Introduction. We consider a perturbed two dimensional Allen-Cahn equation, boundary layer analysis

$$\begin{cases} u_t = \varepsilon^2 \Delta u + f(u) + \varepsilon g(u), & x \in \Omega \subset \mathbb{R}^2, \\ \partial_n u = 0, & x \in \partial\Omega. \end{cases} \quad (1.1)$$

Here, Ω is a smooth two-dimensional domain and $f(u)$ is a smooth function having the following properties:

1. f has three roots $u_- < u_0 < u_+$ with $f'(u_{\pm}) < 0$
2. $\int_{u_-}^{u_+} f(u) du = 0$

and $g(u)$ is any smooth function with $\int_{u_-}^{u_+} g(u) du \neq 0$.

The standard Allen-Cahn equation corresponds to $g = 0$, $f = -2u(u^2 - 1)$. This model was introduced in [2] as a simple model of evolution of antiphase boundaries and is now well understood. In the limit $\varepsilon \rightarrow 0$, the solution forms a sharp interface layer. On one side of the interface, $u \sim u_-$ while on the other, $u \sim u_+$. Once the interface layer is formed, its motion is described by the mean curvature law which minimizes the perimeter of the interface ([5], [9]). The stable stationary solution corresponds to an interface with a minimal perimeter that intersects the boundary orthogonally ([12]). Therefore any non-trivial stable steady equilibrium of the unperturbed Allen-Cahn equation consists of a straight interface. The stability of such an interface has been analysed by several authors in variety of settings, see for instance [1], [10], [11], [14], [15], [17]. The main result is that such an interface can be stable provided the domain contains a “neck”. More precisely, as shown in [10], [11], in the limit $\varepsilon \rightarrow 0$, the interface stability depends only on the curvatures κ_+ , κ_- of the boundary at the two points that intersect the interface, and the interface length ℓ . The interface is stable provided that $\ell + \kappa_+^{-1} + \kappa_-^{-1} < 0$. Geometrically, the threshold case corresponds to the two boundaries that are locally concentric.

*Dalhousie University, Department of Mathematics and Statistics

†Chinese University of Hong Kong, Department of Mathematics

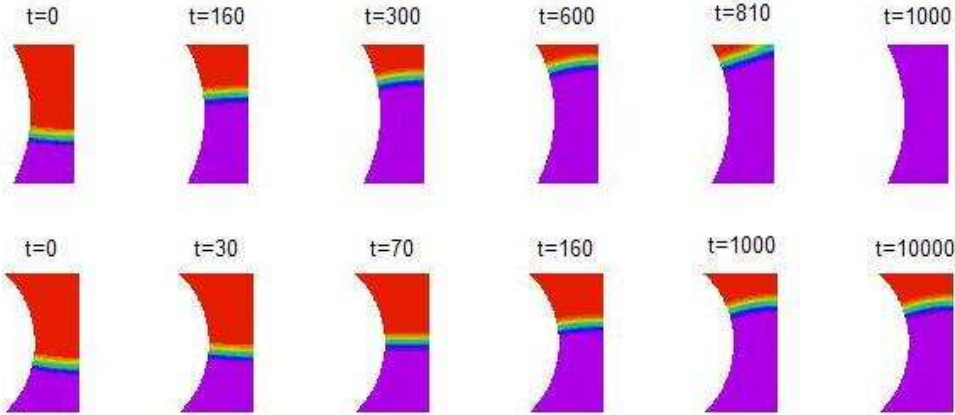


FIG. 1.1. Motion of an interface for the perturbed Allen Cahn model given by $u_t = \varepsilon^2 \Delta u - 2(u - \varepsilon a)(u^2 - 1)$, with $a = 0.3, \varepsilon = 0.07$. Top row: the interface is unstable and eventually disappears. Bottom row: The interface gets “stuck” in the middle of the domain; a non-trivial equilibrium is reached. The domain height is 1.5 and the distance between the side boundaries is 0.5. The radius of the left boundary is 1.5 for the top row and 1.0 for the bottom row.

More generally, the perturbed Allen-Cahn equation (1.1) is used as a prototype model of wave propagation in various contexts. A typical nonlinearity is $f + \varepsilon g = -2(u - A)(u^2 - 1)$ where A is close to 0. This system (but without the assumption that A is small) was used as a simple model of spreading depressions in the human brain that are associated with cerebral strokes [4]. (When A is replaced by an inhomogeneous term $a(x)$, it is called Fife-Greenlee problem [8], [6].) For convex domains, it is known ([3] [13]) that the only stable solution is a trivial equilibrium. Indeed any interface propagates until it merges with the boundary and disappears. However when domain consists of two boxes of different heights, it was shown in [4] that the interface can get “stuck” at the juncture between the two boxes, provided their dimensions are sufficiently different. A similar phenomenon was reported in [16], where the propagation of chemical pulses in complex geometries with corners and junctures was studied numerically and experimentally.

The perturbation by a small term $\varepsilon g(u)$ has a large effect on the shape and stability of the interface. In particular, the equilibrium solution now consists of a *curved* interface. In the limit $\varepsilon \rightarrow 0$, this curve is part of a circular arc whose radius \hat{R} , given by (1.2) below and is independent of the domain shape. For non-convex domains, it is possible to get a stable interface. One such domain is illustrated on Figure 1. It consists of a rectangle with a circular cutout. In the first simulation (top row), the interface propagates through the domain without reaching any equilibrium whereas in the second simulation (second row) the interface settles to a steady state somewhere in the middle of the domain. The only difference between the two simulations is the curvature of the left boundary of the domain, which has been increased in the second simulation.

In this paper, we fully characterize the stability of curved interfaces. First, we provide the necessary and sufficient conditions that describe the stability of an interface. Second, we give a simple geometric interpretation of our stability results.

Before stating our stability result, we characterize the radius of the steady state. This simple result was already given in [15], Appendix A. We summarize it here as

following.

PROPOSITION 1.1. *Let U be a solution to*

$$U''(y) + f(U) = 0, \quad U \rightarrow u_{\pm} \quad \text{as } y \rightarrow \pm\infty$$

and define

$$\hat{R} = -\frac{\int_{-\infty}^{\infty} U'^2(y) dy}{\int_{u_-}^{u_+} g(u) du}. \quad (1.2)$$

Suppose that there exists a circle of radius \hat{R} which intersects $\partial\Omega$ orthogonally, and let p be its center. Then in the limit $\varepsilon \rightarrow 0$ we have

$$u(x) \sim U\left(\frac{\hat{R} - |p - x|}{\varepsilon}\right), \quad \varepsilon \rightarrow 0 \quad (1.3)$$

Moreover, any solution to (1.1) of the form (1.3) must satisfy (1.2).

We are now ready to state our main result.

THEOREM 1.2. *Let $u(x)$ be the steady-state solution as given in Proposition 1.1 and \hat{R} its radius as defined in (1.2). Let ℓ be the length of the interface and let κ_+, κ_- be the curvatures of the boundary at the points which intersect the interface. Consider the stability problem associated with (1.1),*

$$\begin{cases} \lambda\phi = \varepsilon^2\Delta\phi + f'(u)\phi + \varepsilon g'(u)\phi, & x \in \Omega \\ \partial_n\phi = 0, & x \in \partial\Omega. \end{cases} \quad (1.4)$$

In the limit $\varepsilon \rightarrow 0$, the eigenvalues λ are of $O(\varepsilon^2)$ given by

$$\lambda = \varepsilon^2\lambda_0 \quad (1.5a)$$

where λ_0 solves the following geometric eigenvalue problem:

$$\begin{cases} T'' + (\hat{R}^{-2} - \lambda_0)T = 0 \\ T'(-\ell/2) + \kappa_-T(-\ell/2) = 0 \\ T'(\ell/2) - \kappa_+T(\ell/2) = 0. \end{cases} \quad (1.5b)$$

Thus, the interface is stable if all solutions λ_0 of (1.5b) are negative, and unstable if at least one solution is positive. Equivalently, λ_0 solves

$$\lambda_0 = \frac{1}{\hat{R}^2} - \mu^2 \quad \text{where} \quad \tan(\mu\ell) = -\frac{\mu(\kappa_+ + \kappa_-)}{\mu^2 - \kappa_+\kappa_-} \quad (1.6)$$

or

$$\arctan\left(\frac{-\kappa_+}{\mu}\right) + \arctan\left(\frac{-\kappa_-}{\mu}\right) = \mu\ell \quad (1.7)$$

for some branch of arctan.

Remark: Suppose that $\lambda_0 \neq 0$, i.e., the geometric eigenvalue problem (1.5b) has no zero eigenvalue. Then the existence of such steady state can be rigorously proved, following the lines of [11]. We omit the details.

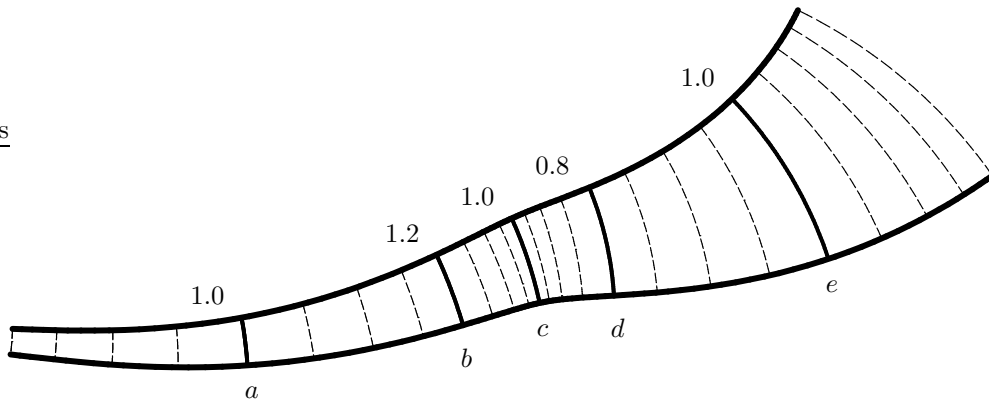


FIG. 1.2. Geometric interpretation of stability criterion (see Theorem 1.3). The numbers indicate the radius of the corresponding interface below that number. The maximum and minimum radius is 1.2 and 0.8, respectively. If $\hat{R} = 1$ then curve c represents the location of a stable interface, whereas curves a and e correspond to unstable interfaces.

In the case of the unperturbed Allen-Cahn equation ($g = 0$, $\hat{R} = \infty$), the geometric eigenvalue problem (1.5b) is identical to Equation (1.5) obtained by Kowalczyk in [10], [11]. However here, we use a somewhat different method using solvability condition and test functions.

The stability criterion (1.5b) has a natural geometric interpretation which we now discuss. Consider a domain such as shown in Figure 1.2. Parameterize the top boundary in terms of arclength s , from left to right, and let $q(s)$ be the corresponding point on the top boundary. We suppose that there is a unique circle that goes through $q(s)$ and that intersects both top and bottom boundaries orthogonally. Let $R(s)$ denote the radius of such a circle. Then we have the following.

THEOREM 1.3. *Let \hat{R} be the radius of a steady interface as defined in Proposition 1.1, let $R(s)$ be as defined above, and suppose that $R(s) = \hat{R}$ for some s . Then the interface is stable if $R'(s) < 0$ and it is unstable if $R'(s) > 0$.*

For example, for the domain as shown in Figure 1.2, if $\hat{R} \in (0.8, 1.2)$ then there exists a stable steady interface between curves b and d . On the other hand, any interface to the left of b or to the right of d is unstable.

The rest of the paper is outlined as follows. Proposition 1.1 is derived in §2. The main result, theorem 1.2 is then derived in §3. Finally we prove Theorem 1.3 in §4. We conclude with numerical calculations in §5 and some discussions and open problems in §6.

2. Equilibrium Front Solution. In this section we construct the steady state consisting of a single interface. The main goal is to derive (1.2) of Proposition 1.1.

We seek a solution which divides the domain into two regions. In one of the regions $u \sim u_+$ and in the other $u \sim u_-$. The two regions are separated by an interface, or front, of thickness $O(\varepsilon)$. We expect the interface to be localized about a circle segment which intersects the boundary of Ω orthogonally. Let \hat{R} be the radius of the interface and define the following coordinate system as illustrated in Figure 2.1:

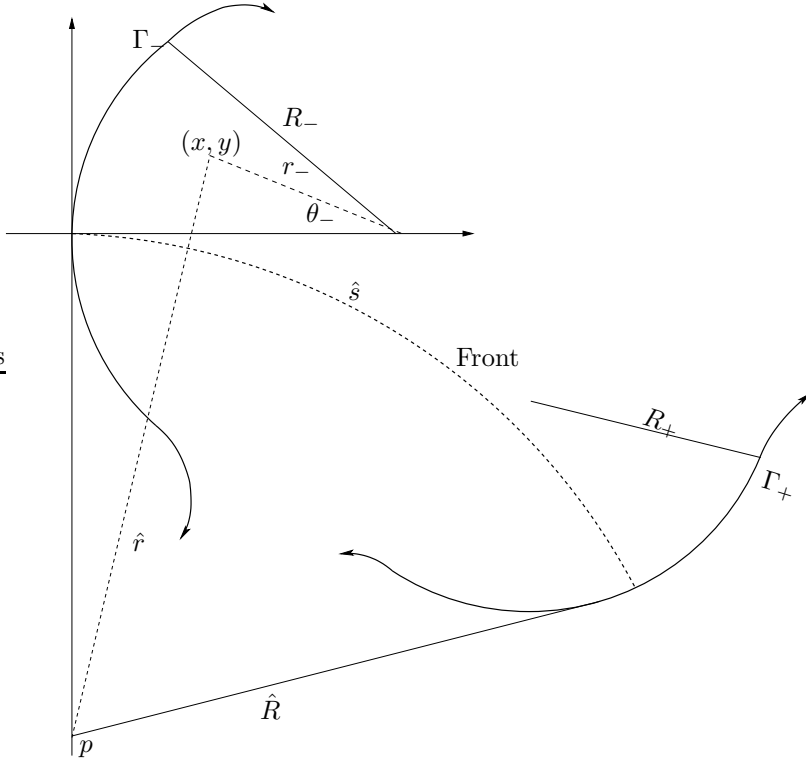


FIG. 2.1. Schematic used for the derivation of coordinate systems in the interior of the domain and localized near the boundaries.

$$x = R_- - r_- \cos(\theta_-) = \hat{r} \sin(\hat{s}/\hat{R}), \quad (2.1)$$

$$y = r_- \sin(\theta_-) = \hat{r} \cos(\hat{s}/\hat{R}) - \hat{R}. \quad (2.2)$$

Near the boundaries, we define localized coordinates ρ_{\pm} and t_{\pm} as follows:

$$\rho_{\pm} \equiv \frac{r_{\pm} - R_{\pm}}{\varepsilon}, \quad t_{\pm} \equiv \frac{R_{\pm}\theta_{\pm}}{\varepsilon}. \quad (2.3)$$

Here, + and - are used to denote the right and left curved boundaries respectively. The \pm will be dropped whenever the meaning is clear. We also define coordinates localized near the front by,

$$\hat{\rho} \equiv \frac{\hat{R} - \hat{r}}{\varepsilon}. \quad (2.4)$$

We can then write $\hat{\rho}$ as a function of t and ρ

$$\hat{\rho} = t - \varepsilon \left(\frac{\rho t}{R} - \frac{\rho^2}{2\hat{R}} \right) + \dots. \quad (2.5)$$

In the interior of the domain, we expect the front to be radially symmetric. Thus in the new coordinate system, the equilibrium front will satisfy

$$u_{\hat{\rho}\hat{\rho}} + \frac{\varepsilon}{\hat{R} + \varepsilon\hat{\rho}} u_{\hat{\rho}} + f(u) + \varepsilon g(u) = 0, \quad (2.6)$$

in the interior of the domain. We expand

$$u = u_0 + \varepsilon u_1 + \varepsilon^2 u_2 + \cdots, \quad (2.7)$$

substitute into (2.6) and collect powers of ε to obtain,

$$u_0'' + f(u_0) = 0, \quad (2.8)$$

$$u_1'' + f'(u_0)u_1 = -\frac{1}{\hat{R}}u_0' - g(u_0), \quad (2.9)$$

$$u_2'' + f'(u_0)u_2 = \frac{1}{\hat{R}^2}\hat{\rho}u_0' - \frac{1}{\hat{R}}u_1' - \frac{f''(u_0)u_1^2}{2} - g'(u_0)u_1. \quad (2.10)$$

From here on ' denotes differentiation with respect to $\hat{\rho}$ when associated with u_i . In all other cases ' will represent differentiation with respect to the appropriate argument. At this point is convenient to define the operator $L\psi \equiv \psi'' + f'(u_0)\psi$.

From conditions 1 and 2 following (1.1) u_0 will be given by the unique heteroclinic orbit connecting u_+ to u_- . For the case $f(u) = 2u(1-u^2)$, we have the exact solution $u_0 = \tanh(\hat{\rho})$. We note that by differentiating (2.8) with respect to $\hat{\rho}$, $Lu_0' = 0$.

To determine \hat{R} , we consider the steady-state system,

$$\varepsilon^2 \Delta u + f(u) + \varepsilon g(u) = 0. \quad (2.11)$$

We multiply (2.11) by u_0' and integrate over the domain,

$$\int_{\Omega} u_0'(\varepsilon^2 \Delta u + f(u) + \varepsilon g(u)) dA = 0. \quad (2.12)$$

Applying Green's identity to (2.12) we obtain

$$-\varepsilon^2 \int_{\partial\Omega} u \partial_n u_0' ds + \int_{\Omega} \varepsilon^2 u \Delta(u_0') + u_0'(f(u) + \varepsilon g(u)) dA = 0. \quad (2.13)$$

We now use (2.7) and (2.4) in (2.13) and collect powers of ε to obtain

$$-\varepsilon^2 \int_{\partial\Omega} u_0 \partial_n u_0' ds + \int_{\Omega} \left((u_0(u_0')'' + f(u_0)u_0') + \varepsilon \left((u_0')''u_1 + \frac{1}{\hat{R}}(u_0')'u_0 + f'(u_0)u_1u_0' + g(u_0)u_0' \right) \right) dA = 0. \quad (2.14)$$

Integrating over $\hat{\rho}$ by parts and using $\lim_{\hat{\rho} \rightarrow \pm\infty} u_0' = 0$ yields

$$\int_{\Omega} (u_0')''u_0 dA = \int_{\Omega} u_0''u_0' dA, \quad (2.15)$$

$$\int_{\Omega} (u_0')'u_0 dA = \int_{\Omega} (u_0')^2 dA. \quad (2.16)$$

Using (2.8) and $Lu_0 = 0$, (2.14) may be written as,

$$-\varepsilon \int_{\partial\Omega} \partial_n u_0' u_0 ds = - \int_{\Omega} \left(\frac{u_0'}{\hat{R}} + g(u_0) \right) u_0' dA. \quad (2.17)$$

Using (2.5) we find the leading order behaviour of $\partial_n u_0'|_{\partial\Omega}$:

$$\partial_n u_0'|_{\partial\Omega} \sim \frac{\partial}{\partial \rho} u_0' \left(t - \varepsilon \left(\frac{\rho t}{R} - \frac{\rho^2}{2\hat{R}} \right) \right) \Big|_{\rho=0}, \quad (2.18)$$

$$= -\varepsilon u_0'' \frac{t}{R}. \quad (2.19)$$

Thus the boundary term in (2.17) is of a much lower order, and the equilibrium radius of the front is given by

$$\hat{R} \sim -\frac{\int_{-\infty}^{\infty} (u'_0)^2 dt}{\int_{u_-}^{u_+} g(y) dy}. \quad (2.20)$$

This shows, that to leading order, \hat{R} is independent of the domain shape and completes the derivation of Proposition 1.1. ■

3. Proof of Theorem 1.2.. We now construct a solvability condition to determine the principal eigenvalues of (1.4). Since u'_0 is of one sign and $Lu'_0 = 0$, we expect that the principal eigenvalue is small and to leading order the principal eigenfunction will behave like u'_0 in the interior of the domain. Such an eigenfunction is often referred to as a translation eigenfunction as it is associated with the near translation invariance of the front in the interior of the domain with respect to the radial co-ordinate. In this case, $\hat{s}u'_0$ also satisfies (1.4) to leading order and as a result, we will need two solvability conditions to determine the principal eigenvalue.

We construct our solvability conditions by multiplying (1.4) by test function v and integrating over the domain we obtain

$$\int_{\Omega} v (\varepsilon^2 \Delta \phi + f'(u) \phi) dA + \varepsilon \int g'(u) \phi v dA = \lambda \int_{\Omega} \phi v dA, \quad (3.1)$$

where v is of the form

$$v(\hat{s}, \hat{\rho}) = w(\hat{s}) u'_0(\hat{\rho}) \quad (3.2)$$

and $w(\hat{s})$ is an arbitrary test function.

Using Green's identity and applying the boundary conditions in (1.4) results in

$$-\varepsilon^2 \int_{\partial\Omega} \phi \partial_n v ds + \int_{\Omega} (\varepsilon^2 \Delta v + f'(u) v + \varepsilon g'(u) v) \phi dA = \lambda \int_{\Omega} \phi v dA. \quad (3.3)$$

Here, s is arc length along the boundary and dA is an element of area in the interior. From (2.3) and (2.4),

$$ds = R d\theta = \varepsilon dt, \quad (3.4)$$

$$dA = \frac{\hat{r}}{\hat{R}} d\hat{r} d\hat{s} = \varepsilon \left(1 + \varepsilon \frac{\hat{\rho}}{\hat{R}} \right) d\hat{\rho} d\hat{s}. \quad (3.5)$$

Consider the $\int_{\Omega} (\varepsilon^2 \Delta v + f'(u) v + \varepsilon g'(u) v) \phi dA$ term in (3.3), in which v , u , ϕ are written in the interior coordinates \hat{r} and \hat{s} . Expand ϕ :

$$\phi = \phi_0 + \varepsilon \phi_1 + \varepsilon^2 \phi_2 + \dots. \quad (3.6)$$

Use (2.4), (3.5), (3.6), and (2.7) to write $\int_{\Omega} (\varepsilon^2 \Delta v + f'(u) v + \varepsilon g'(u) v) \phi dA$ in terms

of the coordinates, $\hat{\rho}$ and \hat{s} :

$$\begin{aligned}
& \left(\varepsilon^2 \Delta v(\hat{r}) + f'(u) v(\hat{r}) + \varepsilon g'(u) v(\hat{r}) \right) \phi dA \\
& \sim \left[\varepsilon^2 \left(\frac{1}{\varepsilon^2} v_{\hat{\rho}\hat{\rho}} + \frac{1}{\hat{R} + \varepsilon \hat{\rho}} \frac{1}{\varepsilon} v_{\hat{\rho}} + v_{\hat{s}\hat{s}} \right) + f'(u_0 + \varepsilon u_1 + \varepsilon^2 u_2) v \right. \\
& \quad \left. + \varepsilon g'(u_0 + \varepsilon u_1 + \varepsilon^2 u_2) v \right] \left[\phi_0 + \varepsilon \phi_1 + \varepsilon^2 \phi_2 \right] \left[\varepsilon \left(1 + \varepsilon \frac{\hat{\rho}}{\hat{R}} \right) d\hat{\rho} d\hat{s} \right] \\
& \sim \left\{ \varepsilon^2 \left[\frac{1}{\hat{R}} v_{\hat{\rho}} \phi_0 + u_1 f''(u_0) v \phi_0 + g'(u_0) v \phi_0 \right] + \right. \\
& \quad \left. + \varepsilon^3 \left[v_{\hat{s}\hat{s}} \phi_0 + u_2 f''(u_0) v \phi_0 + \frac{1}{2} u_1^2 f'''(u_0) v \phi_0 + u_1 g''(u_0) v \phi_0 \right. \right. \\
& \quad \left. \left. + \frac{1}{\hat{R}} v_{\hat{\rho}} \phi_1 + u_1 f''(u_0) v \phi_1 + g'(u_0) v \phi_1 \right. \right. \\
& \quad \left. \left. + \frac{\hat{\rho}}{\hat{R}} u_1 f''(u_0) v \phi_0 + \frac{\hat{\rho}}{\hat{R}} g'(u_0) v \phi_0 \right] \right\} d\hat{\rho} d\hat{s} \tag{3.7}
\end{aligned}$$

since $v = w(\hat{s})u'_0(\hat{\rho})$ is in the kernel of L .

Equation (3.7) has terms involving u_1 and u_2 , so we must examine the equations (2.9) and (2.10) for these terms. We take the derivative of (2.9) with respect to $\hat{\rho}$ and multiply by ϕ_0 , integrate and use Green's identity to obtain

$$-\int_{\partial\Omega} \partial_n u'_1 \phi_0 ds = \int_{\Omega} \left(-\frac{1}{\hat{R}} u''_0 - f''(u_0) u'_0 u_1 - g'(u_0) u'_0 \right) \phi_0 dA. \tag{3.8}$$

It will become evident that $\lambda = O(\varepsilon^2)$. To avoid tedious calculations, we will write $\lambda = \varepsilon^2 \lambda_0 + \dots$. In this way, λ_0 terms will enter at the correct order. We substitute (3.4) and (3.5) into (3.8) multiply by ε and arrange the terms to match the u_1 term in (3.7):

$$\begin{aligned}
\varepsilon^2 \int_{\Omega} f''(u_0) u'_0 u_1 \phi_0 d\hat{\rho} d\hat{s} &= -\varepsilon^2 \left(\int_{\Omega} \left(\frac{1}{\hat{R}} u''_0 + g'(u_0) u'_0 \right) \phi_0 d\hat{\rho} d\hat{s} + \int_{\partial\Omega} \partial_n u'_1 \phi_0 dt \right) \\
&+ \varepsilon^3 \int_{\Omega} \left(-\frac{1}{\hat{R}} u''_0 - f''(u_0) u'_0 u_1 - g'(u_0) u'_0 \right) \frac{\hat{\rho}}{\hat{R}} \phi_0 d\hat{\rho} d\hat{s} + \dots.
\end{aligned} \tag{3.9}$$

We repeat the above procedure to handle the u_2 term in (3.7). First we differentiate (2.10) with respect to $\hat{\rho}$,

$$\Delta(u'_2) + f'(u_0) u'_2 = -\frac{1}{\hat{R}} u''_1 + \frac{1}{\hat{R}^2} \hat{\rho} u''_0 + \frac{1}{\hat{R}^2} u'_0 - f''(u_0) u'_0 u_2 - \frac{f'''(u_0) u'_0 u_1^2}{2} - f''(u_0) u_1 u'_1 - g''(u_0) u'_0 u_1 - g'(u_0) u'_1. \tag{3.10}$$

We multiply the above expression by ϕ_0 , integrate over the domain, apply Green's identity to the right hand side, and multiply by ε^3 to match the u_2 term in (3.7)

which results in the following:

$$\begin{aligned} \varepsilon^3 \int_{\Omega} f''(u_0) u'_0 u_2 \phi_0 \, d\hat{\rho} \, d\hat{s} &= \varepsilon^3 \int_{\Omega} \left(-\frac{1}{\hat{R}} u''_1 + \frac{1}{\hat{R}^2} \hat{\rho} u''_0 + \frac{1}{\hat{R}^2} u'_0 - \frac{f'''(u_0) u'_0 u_1^2}{2} \right. \\ &\quad \left. - f''(u_0) u_1 u'_1 - g''(u_0) u'_0 u_1 - g'(u_0) u'_1 \right) \phi_0 \, d\hat{\rho} \, d\hat{s} \\ &\quad + \varepsilon^3 \int_{\partial\Omega} \partial_n u'_2 \phi_0 \, dt + \dots \end{aligned} \quad (3.11)$$

Since ϕ is a translation eigenfunction, in the interior we may write

$$\phi_i = T(\hat{s}) u'_i(\hat{\rho}). \quad (3.12)$$

We also note that,

$$\int_{\Omega} \frac{1}{\hat{R}} u''_1 \phi_0 \, d\hat{\rho} \, d\hat{s} = - \int_{\Omega} \frac{1}{\hat{R}} \phi'_0 u'_1 \, d\hat{\rho} \, d\hat{s}. \quad (3.13)$$

Using (3.13), (3.12), (3.11), (3.9) and (3.7) we can write (3.1) as

$$\varepsilon^2 \lambda_0 \int_{\Omega} v \phi_0 \, d\hat{\rho} \, d\hat{s} = \varepsilon^2 \int_{\Omega} \left(v_{\hat{s}\hat{s}} \phi_0 + \frac{2}{\hat{R}} \phi_1 v_{\hat{\rho}} + \frac{1}{\hat{R}^2} u'_0 \phi_0 \right) \, d\hat{\rho} \, d\hat{s} - \varepsilon^2 \int_{\partial\Omega} (\phi_0 \partial_n v + \phi_0 \partial_n u'_1) \, dt + \dots \quad (3.14)$$

where, from (3.11), the boundary integral involving $\partial_n u'_2$ is of higher order. The eigenfunction $\phi_0 = T(\hat{s}) u'_0$ is the derivative of a monotonic front and is thus of one sign and hence is the principal eigenfunction. The principal eigenfunction of L must be even in the radial direction and the function v' will be odd in the radial direction. Thus the term $\int_{\Omega} \frac{2}{\hat{R}} \phi_1 v' \, d\hat{\rho} \, d\hat{s}$ will be zero to leading order.

For the boundary integral involving $\partial_n v$, we need to find $\partial_n v$ on $\partial\Omega$. Away from the points where the front and boundary intersect, $\partial_n v$ will be exponentially small, so we will only consider the two components of the boundary Γ_{\pm} . Since the front meets Γ_{\pm} orthogonally,

$$\partial_n v|_{\Gamma_{\pm}} = \pm \frac{\partial v}{\partial r_{\pm}} \Big|_{\Gamma_{\pm}}. \quad (3.15)$$

We note from (2.1), (2.2), (2.3) and (2.4),

$$\frac{\partial \hat{s}}{\partial r} \Big|_{\Gamma_{\pm}} \sim -1 \quad \text{and} \quad \frac{\partial \hat{\rho}}{\partial r} \Big|_{\Gamma_{\pm}} \sim \frac{t}{R}. \quad (3.16)$$

Thus,

$$\partial_n v|_{\Gamma_{\pm}} \sim \left(\mp w'(\hat{s}) u'_0(t) \pm w(\hat{s}) u''_0(t) \frac{t}{R} \right) \Big|_{\Gamma_{\pm}}. \quad (3.17)$$

We let ℓ be the length of the interface and place $\hat{s} = 0$ such that $\hat{s} = \pm\ell/2$ on Γ_{\pm} . Then, using (3.12), (3.2), $\hat{\rho} \sim t$ on Γ_{\pm} and $\int t u''_0 u_0 = -\frac{1}{2} \int u'_0{}^2$ with (3.17) results in,

$$\begin{aligned} - \int_{\partial\Omega} \partial_n v \phi_0 \, dt &\sim - \left(w'(-\ell/2) T(-\ell/2) \int_{-\infty}^{\infty} (u'_0(t))^2 \, dt - \frac{w(-\ell/2) T(-\ell/2)}{2R_-} \int_{-\infty}^{\infty} (u'_0(t))^2 \, dt \right. \\ &\quad \left. - w'(\ell/2) T(\ell/2) \int_{-\infty}^{\infty} (u'_0(t))^2 \, dt - \frac{w(\ell/2) T(\ell/2)}{2R_+} \int_{-\infty}^{\infty} (u'_0(t))^2 \, dt \right). \end{aligned} \quad (3.18)$$

For the boundary integral involving $\partial_n u'_1$, we have that, near $\partial\Omega$,

$$u \sim u_0(\hat{\rho}) + \varepsilon u_1 = u_0(t) - \varepsilon \left(\frac{\rho t}{R} - \frac{\rho^2}{2\hat{R}} \right) u'_0(t) + \varepsilon u_1 + \dots \quad (3.19)$$

Also, on $\partial\Omega$, we have $\partial_n u = 0$, so that, on $\partial\Omega$

$$\partial_n u_1 \sim - \frac{\partial}{\partial \rho} \left[\frac{1}{\varepsilon} u_0(t) - \left(\frac{\rho t}{R} - \frac{\rho^2}{2\hat{R}} \right) u'_0(t) \right] \Big|_{\rho=0} = \frac{t}{R} u'_0(t). \quad (3.20)$$

Then

$$\partial_n u'_1 \sim \frac{1}{R} u'_0(t) + \frac{t}{R} u''_0(t) \quad (3.21)$$

and

$$\begin{aligned} - \int_{\partial\Omega} \partial_n u'_1 \phi \, dt &\sim \int_{\Gamma_-} T(-\ell/2) \left(u''_0(t) u'(t) \frac{t}{R} + u'_0(t)^2 \frac{1}{R} \right) dt \\ &\quad + \int_{\Gamma_+} T(\ell/2) \left(u''_0(t) u'(t) \frac{t}{R} + u'_0(t)^2 \frac{1}{R} \right) dt, \\ &= \left(\frac{T(\ell/2)}{2R_+} + \frac{T(-\ell/2)}{2R_-} \right) \int_{-\infty}^{\infty} (u'_0(t))^2 dt. \end{aligned} \quad (3.22)$$

Substitute (3.17) and (3.22) into (3.14) to obtain

$$\begin{aligned} \left(\lambda_0 - \frac{1}{\hat{R}^2} \right) \int_{\Omega} v \phi_0 \, d\hat{\rho} \, d\hat{s} &\sim \int_{\Omega} v_{\hat{s}\hat{s}} \phi_0 + \left(-w'(-\ell/2)T(-\ell/2) + \frac{w(-\ell/2)T(-\ell/2)}{2R_-} \right. \\ &\quad \left. + w'(\ell/2)T(\ell/2) + \frac{w(\ell/2)T(\ell/2)}{2R_+} + \frac{T(\ell/2)}{2R_+} + \frac{T(-\ell/2)}{2R_-} \right) \int_{-\infty}^{\infty} (u'_0(t))^2 dt. \end{aligned} \quad (3.23)$$

The eigenfunctions will depend on both \hat{s} and $\hat{\rho}$. We thus substitute the ansatz $\phi = T(\hat{s})\Phi(\hat{\rho})$ into the eigenvalue problem (1.4),

$$\left(\Phi'' + \frac{\varepsilon}{\hat{R}} \Phi' - \varepsilon^2 \frac{\hat{\rho}}{\hat{R}^2} \Phi' + f'(u)\Phi + \varepsilon g'(u)\Phi \right) T + \varepsilon^2 T'' \Phi = \varepsilon^2 \lambda_0 T \Phi. \quad (3.24)$$

We divide both sides by $T\Phi$,

$$\left(\frac{\Phi'' + \frac{\varepsilon}{\hat{R}} \Phi' - \varepsilon^2 \frac{\hat{\rho}}{\hat{R}^2} \Phi' + f'(u)\Phi + \varepsilon g'(u)\Phi}{\Phi} \right) + \varepsilon^2 \frac{T''}{T} = \varepsilon^2 \lambda_0. \quad (3.25)$$

Since T is independent of $\hat{\rho}$, the term in the brackets must be independent of $\hat{\rho}$ or equal to a constant α :

$$\Phi'' + \frac{\varepsilon}{\hat{R}} \Phi' - \varepsilon^2 \frac{\hat{\rho}}{\hat{R}^2} \Phi' + f'(u)\Phi + \varepsilon g'(u)\Phi = \alpha \Phi. \quad (3.26)$$

We expand $\Phi = \Phi_0 + \varepsilon \Phi_1 + \varepsilon^2 \Phi_2 + \dots$ and $\alpha = \alpha_0 + \varepsilon \alpha_1 + \varepsilon \alpha_2 + \dots$. The lowest order terms satisfy

$$\Phi_0'' + f'(u_0)\Phi_0 = \alpha_0 \Phi_0. \quad (3.27)$$

Thus $\Phi_0 = u'_0(\hat{\rho})$ and $\alpha_0 = 0$. The $O(\varepsilon)$ terms satisfy

$$\Phi_1'' + f'(u_0)\Phi_1 = \alpha_1\Phi_0 - \frac{1}{\hat{R}}\Phi_0' - f''(u_0)u_1\Phi_0 - g'(u_0)\Phi_0. \quad (3.28)$$

Differentiating (2.9) results in the following solvability condition,

$$\int_{-\infty}^{\infty} f''(u_0)u_1(u'_0)^2 d\hat{\rho} = - \int_{-\infty}^{\infty} g'(u_0)(u'_0)^2 d\hat{\rho}. \quad (3.29)$$

Applying (3.29) to the solvability condition for (3.28), yields $\alpha_1 = 0$. The $O(\varepsilon^2)$ terms satisfy

$$\Phi_2'' + f'(u_0)\Phi_2 = \alpha_2\Phi_0 - \Phi_1' \frac{1}{\hat{R}} + \frac{1}{\hat{R}^2}\hat{\rho}\Phi_0'' - f''(u_0)u_1\Phi_1 - f''(u_0)u_2\Phi_0 - \frac{1}{2}f'''(u_0)u_1^2\Phi_0 - g''(u_0)u_1\Phi_0 - g'(u_0)\Phi_1. \quad (3.30)$$

We have the following solvability condition

$$\begin{aligned} \alpha_2 \int_{-\infty}^{\infty} \Phi_0^2 d\hat{\rho} &= \frac{1}{2} \int_{-\infty}^{\infty} f'''(u_0)u_1^2\Phi_0^2 d\hat{\rho} + \int_{-\infty}^{\infty} g''(u_0)u_1\Phi_0^2 d\hat{\rho} + \int_{-\infty}^{\infty} g'(u_0)\Phi_1\Phi_0 d\hat{\rho} + \int_{-\infty}^{\infty} f''(u_0)u_2\Phi_0^2 d\hat{\rho} + \\ &\int_{-\infty}^{\infty} f''(u_0)u_1\Phi_1\Phi_0 d\hat{\rho} - \int_{-\infty}^{\infty} \frac{1}{\hat{R}^2}\hat{\rho}\Phi_0''\Phi_0 d\hat{\rho} + \int_{-\infty}^{\infty} \frac{1}{\hat{R}}\Phi_1'\Phi_0 d\hat{\rho}. \end{aligned} \quad (3.31)$$

Differentiating (2.10) results in the solvability condition,

$$\begin{aligned} & - \int_{-\infty}^{\infty} f''(u_0)u_2(u'_0)^2 d\hat{\rho} - \int_{-\infty}^{\infty} \frac{1}{\hat{R}}u_1''u'_0 d\hat{\rho} + \frac{1}{\hat{R}^2} \int_{-\infty}^{\infty} \hat{\rho}u_0''u'_0 d\hat{\rho} + \frac{1}{\hat{R}^2} \int_{-\infty}^{\infty} (u'_0)^2 d\hat{\rho} \\ & - \int_{-\infty}^{\infty} f''(u_0)u_1u_1'u'_0 d\hat{\rho} - \frac{1}{2} \int_{-\infty}^{\infty} f'''(u_0)u_1^2(u'_0)^2 d\hat{\rho} - \int_{-\infty}^{\infty} g''(u_0)u_1(u'_0)^2 d\hat{\rho} - \int_{-\infty}^{\infty} g'(u_0)u_1'u'_0 d\hat{\rho} = 0. \end{aligned} \quad (3.32)$$

Now we use $\int_{-\infty}^{\infty} \hat{\rho}u_0''u'_0 d\hat{\rho} = -\frac{1}{2} \int_{-\infty}^{\infty} (u')^2 d\hat{\rho}$ and (3.32) in (3.31) to yield

$$\alpha_2 = \frac{1}{\hat{R}^2}. \quad (3.33)$$

Now we can substitute (3.26) into (3.25) using $\alpha = \frac{\varepsilon^2}{\hat{R}^2} + \dots$ to get

$$T'' = \left(\lambda_0 - \frac{1}{\hat{R}^2} \right) T. \quad (3.34)$$

Note that

$$\left(\lambda_0 - \frac{1}{\hat{R}^2} \right) \int_{\Omega} v\phi_0 d\hat{\rho} d\hat{s} \sim \left(\lambda_0 - \frac{1}{\hat{R}^2} \right) \int_{-\ell/2}^{\ell/2} wTd\hat{s} \int_{-\infty}^{\infty} (u'_0(t))^2 dt \quad (3.35)$$

$$\int_{\Omega} v_{\hat{s}\hat{s}}\phi_0 \sim \int_{-\ell/2}^{\ell/2} w''Td\hat{s} \int_{-\infty}^{\infty} (u'_0(t))^2 dt. \quad (3.36)$$

Substituting (3.34), (3.35) and (3.36) into (3.23), integrating by parts, we obtain

$$w(-\ell/2) \left[T'(-\ell/2) + \frac{1}{\hat{R}_-} T(-\ell/2) \right] + w(\ell/2) \left[-T'(\ell/2) + \frac{1}{\hat{R}_+} T(\ell/2) \right] = 0.$$

Since w is an arbitrary test function, we see that T satisfies the following boundary conditions

$$T'(-\ell/2) + \frac{1}{R_-}T(-\ell/2) = 0, \quad -T'(\ell/2) + \frac{1}{R_+}T(\ell/2) = 0. \quad (3.37)$$

(3.34) and (3.37) proves that T satisfies the geometric eigenvalue problem (1.5b). Hence $\lambda_0 = \frac{1}{R^2} - \alpha$ where α satisfies

$$\begin{cases} T'' + \alpha T = 0 \\ T'(-\ell/2) + \kappa_- T(-\ell/2) = 0 \\ T'(\ell/2) - \kappa_+ T(\ell/2) = 0, \end{cases} \quad (3.38)$$

where, $\kappa_{\pm} \equiv \frac{1}{R_{\pm}}$ and $\kappa_{\pm} > 0$ corresponds to a convex domain as in Figure 2.1.

If $\alpha \leq 0$, then $\lambda_0 \geq \frac{1}{R^2}$. If $\alpha = \mu^2 > 0$, (where $\mu > 0$), then it is easy to see that μ must satisfy the following transcendental relation:

$$\tan(\mu\ell) = \frac{\mu(\kappa_+ + \kappa_-)}{\kappa_+\kappa_- - \mu^2}, \quad (3.39)$$

and the eigenvalues of (1.4) are given by,

$$\varepsilon^2\lambda = \frac{1}{R} - \mu^2, \quad (3.40)$$

which is precisely (1.6). Formula (1.7) is seen to be identical to (1.6) by applying the identity

$$\tan(x+y) = \frac{\tan x + \tan y}{1 - \tan x \tan y} \quad (3.41)$$

This completes the proof of Theorem 1.2. ■

4. Proof of Theorem 1.3.. In this section we show that geometric condition of Theorem 1.3 is a direct consequence of Theorem 1.2.

Fix a point q_+ on the top boundary and consider a circular arc going through q_+ and intersecting both top and bottom boundaries orthogonally (refer to Figure 4.1). Let p be the center of this arc and let R denote its radius. First, we shall show that $\frac{dR}{dq_+} = 0$ if and only if the formula (1.5) holds with $\lambda_0 = 0$. By zooming into the point where $\frac{dR}{dq_+} = 0$, we can assume that locally, p moves along a straight line as q_+ moves along the boundary, and that the boundaries are segments of circles of radii \mathcal{R}_{\pm} , as shown on Figure 4.1. In general, \mathcal{R}_{\pm} may be positive or negative; for convenience, as shown on the figure, we chose $\mathcal{R}_{\pm} = -\frac{1}{\kappa_{\pm}}$ with $\kappa_{\pm} < 0$ so that \mathcal{R}_{\pm} are positive. Now from geometry, we find the relationship

$$R = \frac{\mathcal{R}_+(1 - \cos\theta_+) + h_+}{\sin\theta_+}.$$

where h_+, θ_+ are as shown on Figure 4.1. We obtain

$$\frac{\partial R}{\partial \theta_+} = \frac{\mathcal{R}_+ - (\mathcal{R}_+ + h_+) \cos\theta_+}{\sin^2\theta_+}$$

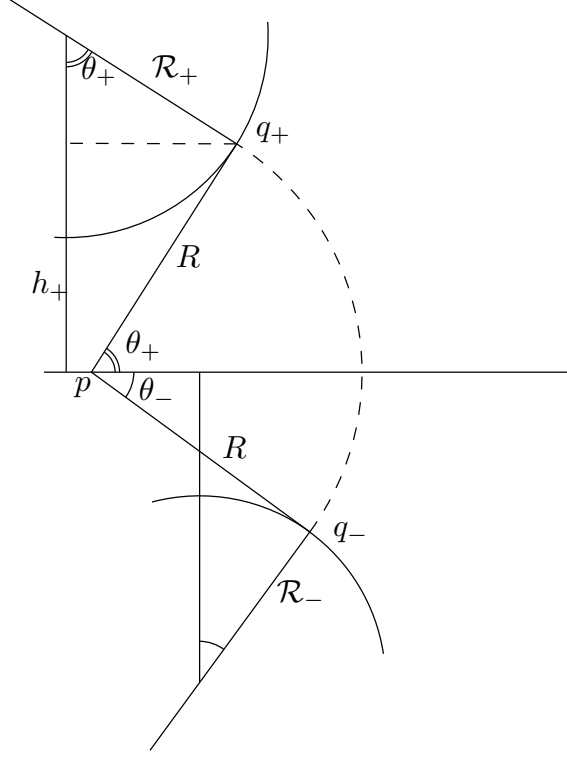


FIG. 4.1. Setup for proof of Theorem 1.3

so that upon eliminating h_+ we obtain

$$\frac{\partial R}{\partial \theta_+} = 0 \iff \frac{R}{\mathcal{R}_+} = \tan \theta_+ \quad (4.1)$$

and similarly with $+$ replaced by $-$. Since θ_{\pm} are functions of q_+ , we find that at the point where $\frac{dR}{dq_+} = 0$, we have

$$\arctan \frac{R}{\mathcal{R}_{\pm}} = \theta_{\pm}.$$

Now from geometry, $\theta_+ = \ell_+/R$, $\theta_- = \ell_-/R$ and $\ell = \ell_+ + \ell_-$. Therefore upon adding the two equations in (4.1) we obtain

$$\arctan \frac{R}{\mathcal{R}_+} + \arctan \frac{R}{\mathcal{R}_-} = \theta_+ + \theta_- = \frac{\ell}{R}.$$

But this is precisely (1.7) with $\lambda_0 = 0$ after substituting $\mathcal{R}_{\pm} = -\frac{1}{\kappa_{\pm}}$.

Next, we note that in the case of a cone ($\kappa_+ = \kappa_- = 0$), equation (1.7) yields $\lambda_0 = \frac{1}{R^2} > 0$ so that the interface is unstable for a cone domain, for which $R' > 0$. Since λ_0 can only be real, it follows by continuity that λ_0 crosses zero if and only if $R' = 0$, and λ_0 is negative if and only if $R' < 0$. This concludes the proof. ■

5. Numerical example. We now provide a numerical example of Theorem 1.2.

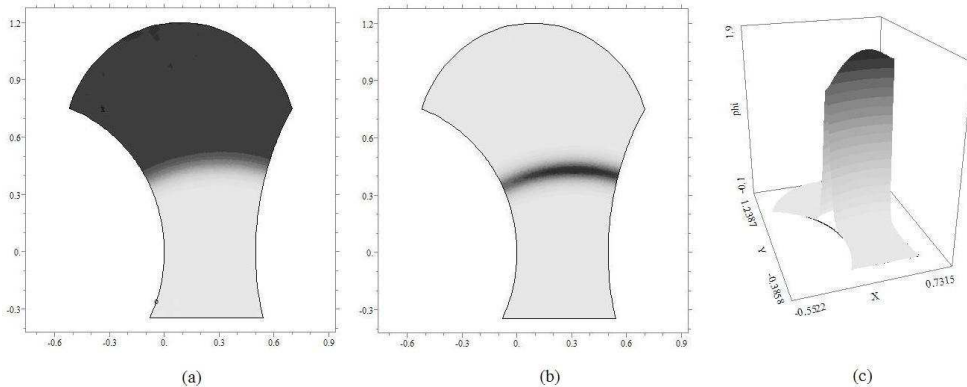


FIG. 5.1. Numerical computation of interface and eigenvalue. Left: the steady-state solution $u(x)$ of (5.1). Dark denotes $u \sim 1$ and light denotes $u \sim -1$. Middle: The shape of the corresponding eigenfunction ϕ . Right: surface plot of ϕ . Note the sinusoidal shape along the direction of the interface boundary. Note also a corner layer that is evident near the boundary of the domain. See §5 for parameter values.

All computations were done using using the software FlexPDE [18].

Consider a domain as shown in Figure 5.1. Its left and right boundaries consist of arcs of circles of radii $\mathcal{R}_- = 0.8$, $\mathcal{R}_+ = 1.5$, so that $\kappa_- = -1.25$, $\kappa_+ = -0.667$. The distance between these two boundaries was chosen to be 0.5. The shape of the top and bottom boundaries does not affect the computation as long as they are located $O(1)$ distance from the interface. We chose the nonlinearity to be

$$u_t = \varepsilon^2 \Delta u - 2(u - \varepsilon a)(u - 1)(u + 1) \quad (5.1)$$

with $a = 0.55$, $\varepsilon = 0.06$. From Proposition 1.1 we obtain the theoretical value of the interface radius to be $\hat{R} = \frac{1}{2a} = 0.9091$. To estimate the numerical value of \hat{R} , we have used FlexPDE to compute the steady state solution to (5.1), using $u = \tanh(y/\varepsilon)$ as initial conditions. The resulting steady state is shown on Figure 5.1.a. Next, we computed the coordinates of the intersection of the middle of the interface ($u = 0$) with the boundary, and then used geometry to obtain $\hat{R}_{\text{numerical}} = 0.9066$. This is in excellent agreement with the theoretical prediction. Geometry then yields an estimate of $l = 0.6486$.

Next, we have solved the eigenvalue problem (1.4) numerically. Using global error tolerance of 0.5×10^{-4} , we obtained a numerical estimate of $\lambda_{\text{numerical}} = 0.00504$. This required about 10000 gridpoints (FlexPDE uses adaptive gridding, and chooses the mesh size based on the global tolerance setting. We have also verified that this result is correct to two significant digits by changing the tolerance). On the other hand solving (1.6) gives the theoretical estimate of $\lambda = 0.00506$. Excellent agreement (within 0.5%) is observed.

6. Discussion.

In this paper we have characterized the stability of curved in-

terfaces in algebraic and geometric terms. Algebraically, this condition is given by Theorem 1.2. It is a generalization of the geometric eigenvalue problem derived in [10], [11]. Geometrically, Theorem 1.3 states that if $R(s)$ denotes the radius of an arc that intersects the boundary orthogonally at $q_{\pm}(s)$, then the interface is stable if $R'(s) < 0$ whenever $R = \hat{R}$, whereas the interface is unstable if $R'(s) > 0$ at that

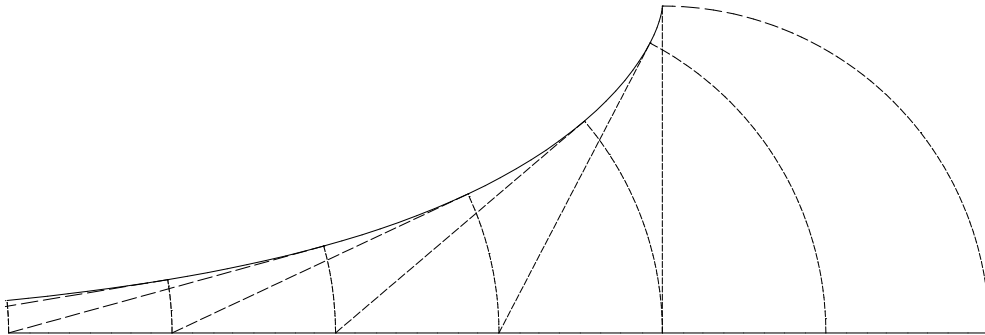


FIG. 6.1. A tractrix: the threshold case where all circles intersecting the boundary have identical radius. Theorem 1.3 does not apply to such a domain.

point (see Figure 1.2). In particular, this shows explicitly the well-known result that an interface at equilibrium cannot be stable in a convex domain; on the other hand we have shown numerical and theoretical examples where such interface is stable when the domain is non-convex.

In general, the relationship between the radius R of a circle that intersects the boundary orthogonally and the domain boundary $q = (x, y)$ is given by

$$x = p_1 + R \cos \theta, \quad y = p_2 + R \sin \theta$$

where $p = (p_1, p_2)$ is the center of the arc of radius R ; p_1, p_2, R are arbitrary functions of s ; and θ satisfies a differential equation

$$R \frac{d\theta}{ds} = p'_1 \sin \theta - p'_2 \cos \theta.$$

An interesting threshold case corresponds to $R = \hat{R}$ for all s . If the bottom boundary is the x-axis and $R = \hat{R}$ for all s , then the top boundary forms a *tractrix* (see Figure 6.1.) This is a well-known curve that is also generated when a ball is dragged on a fixed string by a tractor moving along the x-axis. Implicitly, this curve is given by

$$x = \hat{R}(-t + \tanh(t)), \quad y = \hat{R} \operatorname{sech}(t).$$

It is an open problem to describe either the stability or the location of the interface for such a domain.

An interesting conjecture arises in study the propagation of fronts around a concave corner. Such domains were used in [16], where the propagation of chemical fronts was considered. An interface passing through the corner may get “stuck” at the corner or go through it, depending on the geometry. If we “smooth out” the corner and take ε sufficiently small, then we can apply Theorem 1.3. The result is that the interface will get stuck at the corner if there exists a circle that intersects orthogonally with one boundary, and that passes through the corner point, and whose radius is at most \hat{R} . This is essentially the geometrical condition described in §III.B in [16] and it agrees well with numerical results presented there. However the construction of an interface at a corner point is an open theoretical problem.

Acknowledgment. The research programs of David Iron and Theodore Kolokolnikov are supported by NSERC Discovery Grants.

REFERENCES

- [1] N.Alikakos, G.Fusco, and M.Kowalczyk, *Finite dimensional dynamics and interfaces intersecting the boundary: Equilibria and the quasi-invariant manifold*, Indiana Univ. Math. J. 45 No. 4 (1996) 1119-1156
- [2] S. Allen and J. W. Cahn, *A microscopic theory for antiphase boundary motion and its application to antiphase domain coarsening*, Acta. Metall. 27 (1979), 1084-1095.
- [3] R.G.Casten and J.Holland, *Instability results for reaction diffusion equations with Neumann boundary conditions*, J.Diff.Eq., Vol. 27(2), (1978), pp. 266-273.
- [4] G.Chapuisat and E.Grenier, *Existence and nonexistence of traveling wave solutions for a bistable reaction-diffusion equation in an infinite cylinder whose diameter is suddenly increased*, Comm.PDE, 30:1805-1816, (2005).
- [5] X. Chen, *Generation and propagation of interfaces in reaction-diffusion equations*, J. Diff. Eqns. 96(1992), 116-141.
- [6] M. del Pino, M. Kowalczyk and J. Wei, *Resonance and interior layers in an inhomogeneous phase transition model*. SIAM J. Math. Anal. 38 (2006/07), no. 5, 1542-1564.
- [7] P.C.Fife, and J.B.MacLeod, *The approach of solutions of nonlinear diffusion equations to travelling front solutions*, Arch Ration Mech Anal 65:335-361 (1977).
- [8] P. Fife and W.M.Greenlee, *Interior transition layers for elliptic boundary value problems with a small parameter*, Russian Math. Surveys 29:4(1974), 103-131.
- [9] T. Ilmanen, *Convergence of the Allen-Cahn equation to the Brakke's motion by mean curvature*, J. Diff. geom. 38(1993), 417-461.
- [10] M. Kowalczyk, *Approximate invariant manifold of the Allen-Cahn flow in two dimensions*, preprint
- [11] M. Kowalczyk, *On the existence and Morse index of solutions to the Allen-Cahn equation in two dimensions*, Ann Mat Pura et Applicata, Vol. 184, No. 1 (March 2005) pp. 0373-3114.
- [12] R. Kohn and P. Sternberg, *Local minimizers and singular perturbations*, Proc. Royal Soc. Edinburgh 111 A (1989), 69-84.
- [13] H. Matano, *Asymptotic behavior and stability of solutions of semilinear diffusion equations*, Publ. Res. Inst. Math. Sci. 15(1979), 401-454.
- [14] F. Pacard and M. Ritore, *From the constant mean curvature hypersurfaces to the gradient theory of phase transition*, J. Diff. Geom., to appear.
- [15] J. Rubinstein, P. Sternberg and J.B. Keller, *Fast reaction, Slow diffusion, and Curve shortening* SIAM J.Appl.Math., Vol. 49, No. 1. (Feb., 1989), pp. 116-133.
- [16] L.Qiao, I.G.Kevrekidis, C.Punctk and H.H.Rotermund, *Guiding chemical pulses through geometry: Y junctions*, Phys.Rev.E 73, 036219 (2006).
- [17] M.Ward and D.Stafford, *Metastable dynamics and spatially inhomogeneous equilibria in dumbbell-shaped domains*, Studies in Applied Math. 103, No. 1, (1999), pp. 51-73.
- [18] See FlexPDE website, www.pdesolutions.com.